phasized the need for some additional means of determining the identity of human skeletal remains. On the basis of rather extensive experience in working with x-ray films of the hands and wrists of children and adults, I had gained the impression that the various skeletal features visible in the posterior-anterior radiograph of the hand and wrist might be found to differ sufficiently from one person to another to permit identification of individuals from these alone. This report summarizes the results of an attempt to determine the usefulness of those radiographic features for this purpose (*1*).

It was established that, as seen in the posterior-anterior radiograph, the various bones of the hand and wrist show individual differences in form and in other features which, in the aggregate, are sufficient to distinguish the radiograph of the hand of one person from that of another. To begin with the ends of the radius and ulna and proceed distally, these features are: (i) the shape and relative size of the distal end of the radius and of the styloid process of the ulna; (ii) the shape of the individual carpal bones; (iii) the size and shape of the individual metacarpals, the relative width of their cortices and medullary cavities, and the individual differences in the outline of the inner margin of the cortex (that is, the margin immediately adjacent to the medullary cavity); (iv) the shape and position of the irregular white lines visible in the heads of the metacarpals; (these lines are composite shadows to which parts of the volar and dorsal surfaces and structures lying between them make variable relative contributions); (v) the differences in the shape and relative dimensions of the individual phalanges; and (vi) the fine details of trabecular pattern visible in the shafts of the various bones, especially in the proximal and middle phalanges.

A study of a series of radiographs of the hand made at regular intervals on the same individuals, from early childhood over a long period of years, disclosed that the skeletal features which are useful for individual identification usually become established during late adolescence and remain relatively unchanged until at least well into the thirties, the age of the oldest men on whom such film series were available to us. Since, however, the same features were observed in radiographs of the hand of several hundred men and women who were in their seventies and eighties, it is thought that most of those features remain recognizable throughout the life of the individual, even though they occasionally become modified somewhat by changes associated with aging.

In the radiograph of the hand and wrist, 27 complete bones and parts of two other bones (the distal ends of the radius and ulna) are visible. Since most of these possess a number of structural features which can differ from one person to another, the chance that radiographs of the hands of any two persons will be identical in all of these features would seem to be very small—if, indeed, such identity ever occurs.

Harold E. Jones, director of the Institute of Child Welfare of the University of California at Berkeley, kindly permitted me to study radiographs of the right and left hands of 70 pairs of like-sexed twins on whom he had previously made some other observations. Approximately 40 of these pairs appeared to be identical twins. While there was a very striking resemblance between x-ray films of the hand of the two members of each presumably identical pair, there were in every instance some features which made it possible to distinguish the hand and wrist bones of one person from those of his or her twin. The over-all similarity was so great, however, and our observations were so few, that we ought not ignore the possibility that skeletal features which we have found adequate to distinguish between radiographs of the hand of unrelated persons and of ordinary siblings are, in some instances, not sufficiently discriminating to distinguish an x-ray film of the hand of one identical twin from that of the other member of the pair. However, as mentioned above, no such instance was encountered among the cases which we were able to study.

In about 500 of the young men whom we x-rayed, separate radiographs were made of both the right and the left hand. Though, as might be expected, an individual bone of one hand or wrist is not always identical in form with the corresponding bone of the other side, it was found that there was a sufficiently close over-all similarity in the shape and proportions of the bones of the two hands to permit successful pairing of the two films of the same man when all identifying marks had been covered and the films were studied in a random order. It should, therefore, be possible to identify skeletal remains in which the bones of the forearm, wrist, and hand of only one side are present, by comparing the radiographic features of these bones with those visible in an x-ray film which had previously been made of the same or of the opposite side.

It might be thought that the ease with which the radiograph of the hand of one person can be distinguished from that of another in our population may, to some extent, be due to the heterogeneity in race and in national antecedents of the people of the United States. Our study of films of the hands of several hundred Apache Indians from the White River Reservation in Arizona and of a larger number of American-born Japanese living in California established, however, that the same individual differences in the skeletal features which we had observed in the more heterogeneous white population in our country exist also among American Indians and Japanese. Radiographs of the hand can, therefore, be used satisfactorily for purposes of individual identification within those groups and, presumably, among other racial groups as well.

These findings demonstrate that it is quite possible to establish the identity of an individual from the skeletal features visible in an x-ray film of his hand and wrist. Since many of those features remain relatively unchanged even after years of burial, the films could also provide conclusive proof of the identity of persons in whose remains other identifiable features are lacking.

WILLIAM WALTER GREULICH
Department of Anatomy, Stanford University School of Medicine, Stanford, California

Note

1. This investigation was supported by the Department of the Army through contract No. DA 19-129-QM-816.

26 August 1959

Electronmicroscopy of Dental Calculus

Abstract. Electron microscopy of ultrathin osmium-fixed sections of dental calculus, cut with a diamond knife without prior decalcification, revealed densely mineralized areas entrapping many degenerating microorganisms, within which were deposited similarly electron-dense crystals. Two principal forms of crystals were found, the predominant type being of the same order of magnitude and shape as those found in bone, and showing the typical characteristics of apatite in selected area electron diffraction patterns.

At present it is not possible to propose a single mechanism sufficiently inclusive to explain calcifiability of such diverse structures as endoskeletons, exoskeletons, teeth, kidney stones, or pearls, to name but a few of many normal and pathological types of calcification in biological systems (*1*). The most attractive conceptual scheme hitherto suggested to account for mineral deposition in vertebrate hard structures of mesodermal origin has evolved from the electron microscopic observations by Robinson (*2*) and Robinson and Watson (*3*), who studied adult human bone and dentin; by Jackson and Randall (*4*), who examined embryonic avian bone; and by Glimcher *et al.* (*5*), who employed an in-vitro system of reconstituted mammalian collagen immersed in metastable phosphate solutions. According to these studies, a precise relationship was found to exist between the ultrastructural axial periodicity (640 A) of the native collagenous fibrous framework and the initial nucleation and ultimate orientation of the apatite crystal lattice.

The present study deals with a calcifiable biological system in which the deposition of bonelike crystals is demonstrated in a matrix independent of the cellular activities and fibrous protein synthesis of skeletal and dental organs, namely, the highly mineralized concretions known as dental calculus, or tartar, deposited within the oral environment on the external exposed surfaces of human teeth.

Recently accumulated concretions of supragingival dental calculus were collected from the lingual surface of the anterior teeth of adult patients who tended to form such deposits repeatedly within a week or two (*6*). Following fixation in 10 percent buffered osmium tetraoxide for 18 hours, the material was embedded in a mixture of 9 parts butylmethacrylate to 1 part methylmethacrylate. Without prior decalcification, sections were cut with a diamond knife and observed in the R.C.A. EMU 3-B electron microscope at 50 kv. Small uniform areas of the sections were subsequently examined by selected area electron diffraction.

At lower power (Fig. 1) a stratification of some calcified areas manifested itself as alternating, irregular bands of greater and lesser electron density. Two types of calcification fronts were observed: one was heavily mineralized and ended abruptly facing a structureless matrix of very low electron density (Fig. 2); the second type was less heavily calcified, more diffuse at its border, and faced a matrix consisting of a feltlike mat apparently containing delicate fibrillar elements (Fig. 3). It would be expected that the former type represented the older and more mature concretions, whereas in the latter the calculus was actively growing and as yet incompletely mineralized.

Within and beyond the areas of calcification the sectioned calculus revealed numerous circular to oblong structures, 0.4 to 0.5 μ in the smaller dimension (Fig. 4), evidently representing crosscut microorganisms. It is known that dental calculus invariably contains a predominance of filamentous organisms, whereas other types of microorganisms, though isolated from calculus, are thought to be transients and not directly involved in calculus formation (*7*).

The organisms seen in the electronmicrographs were either completely entombed within solidly calcified bodies (Fig. 4), or outside calcified bodies within a homogeneous matrix of very low electron density (Fig. 2). Organisms found within calcified areas were in various stages of degeneration. The crystals of mineral, initially occurring in spaces between organisms (Fig. 4), eventually occurred within organisms or the spaces remaining after they degenerated (Fig. 3).

The inorganic crystals were of two principal size classes: (i) very large crystals measuring about 500 by 26,000 A (Fig. 5), and, predominantly, (ii) very fine, more or less randomly oriented crystallites measuring about 40 by 800 A, of the same order of magnitude as those in bone (compare Figs. 6 and 7).

So far we have not attempted a systematic characterization of the mineral deposits, except to indicate that the principal crystal form has the electron diffraction pattern of apatitie (Fig. 8). This direct visualization of crystals simulating typical bone salts is in keeping with chemical and x-ray diffraction studies, recently reviewed by Leung and Tovborg Jensen (*7*), according to which hydroxyapatite is always present in calculus. The admixture of other types of crystals observed in the electronmicrographs may be related to the finding that up to 60 percent of brushite ($CaHPO_4$, $2H_2O$) may be found in certain specimens of supragingival calculus from the anterior mandibular teeth (*8*), the same origin as that of calculus examined in the present study, and to the finding that 80 percent of dental calculus deposits contain whitlockite [$Ca_3(PO_4)_2$]. In these crystals the substitution with magnesium has been considered a factor which in part may inhibit the growth of the otherwise predominant apatite (*8, 9*).

While microorganisms have been implicated in formation and attachment of calculus, it is believed that the above observations for the first time indicate that these organisms themselves may be subject to mineral deposition. In this connection, it is interesting to note that

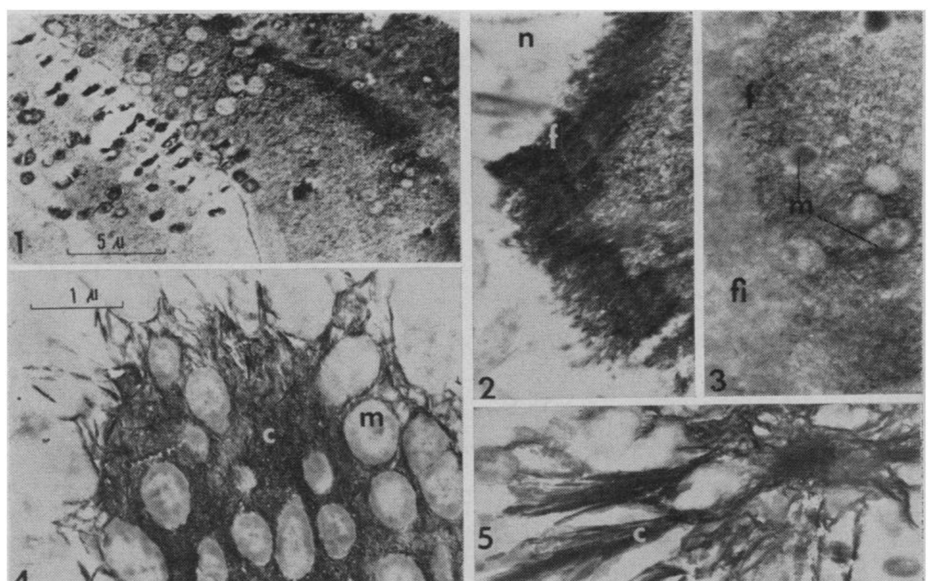

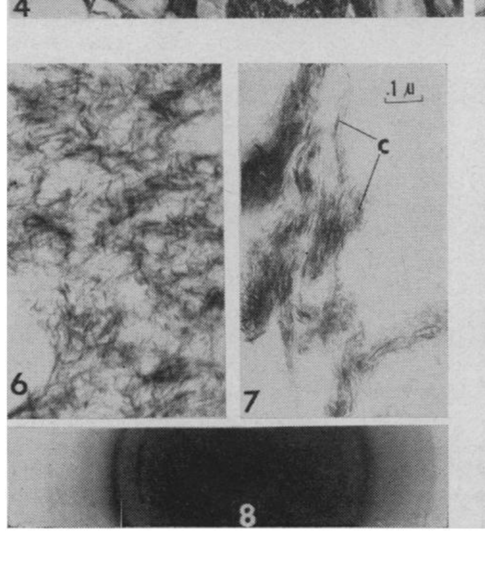

Figs. 1–6. Electron micrographs of ultrathin sections of undecalcified dental calculus. At low power (Fig. 1), the calcified area shows stratification and entrapped microorganisms in various stages of degeneration and calcification. Figs. 2 and 3 show two types of calcification fronts. In some regions (Fig. 2) microorganisms are seen outside the calcified area; other organisms (Fig. 3) are seen with crystals within them. In Fig. 4 can be seen microorganisms completely surrounded by a network of crystalline material. An example of the larger class of crystals is shown in Fig. 5, finer crystals in Fig. 6. Figs. 7 and 8. The minute predominant crystals of calculus are of the same order of magnitude as those found in bone (Fig. 7) and exhibit the electron diffraction pattern characteristic of apatite (Fig. 8). Magnifications: Fig. 1, × 2500; Figs. 2–5, × 11,300; Figs. 6 and 7, × 46,500. Key: n, homogeneous matrix; fi, fibrillar matrix; f, calcification front; m, microorganism; c, inorganic crystals.

Pautard (*10*) has found, in *Spirostomum ambiguum*, a ciliated protozoan, intracellular deposition of apatite "bone" salts with an x-ray diffraction pattern indistinguishable from that of extracellular mesodermal hard tissue matrices.

Evidently, the "matrix" outside of the microorganisms represents the bulk of the calcified deposits; but it is not known to what extent the microorganisms contribute to the conversion of this initially amorphous substance, presumably salivary mucus, into a calcifiable framework. The nature of this matrix is basic to a fuller understanding of apatite nucleation in biological systems (*11*).

F. GONZALES*
R. F. SOGNNAES
Harvard School of Dental Medicine, Boston, Massachusetts

References and Notes

1. R. F. Sognnaes, Ed., *Calcification in Biological Systems* (American Association for the Advancement of Science, Washington, D.C., in press.)
2. R. A. Robinson, *J. Bone and Joint Surg.* **34A**, 389 (1952).
3. R. A. Robinson and M. L. Watson, *Ann. N.Y. Acad. Sci.* **60**, 596 (1955).
4. S. F. Jackson and J. T. Randall, in *Bone Structure and Metabolism* (Little, Brown, Boston, 1956), pp. 47 ff.
M. F. Glimcher, A. J. Hodge, F. O. Schmitt, *Proc. Natl. Acad. Sci. U.S.* **43**, 860 (1957).
6. Specimens of dental calculus were kindly provided by Dr. Paul Goldhaber.
7. S. W. Leung and A. Tovborg Jensen, *Intern. Dental J.* **8**, 613 (1958).
8. A. Tovborg Jensen and M. Danö, *J. Dental Research* **33**, 741 (1954).
9. ——— and S. L. Rowles, *Acta Odontol, Scand.* **15**, 121 (1957).
10. F. G. E. Pautard, *Biochim. et Biophys. Acta* **28**, 514 (1958); "Calcification in unicellular organisms," in *Calcification in Biological Systems* (*1*).
11. This study was aided by grants from the U.S. Public Health Service (D-662) and from the William F. Milton Fund and Higgins Trust of Harvard University.
* U.S. Public Health Service senior research fellow (SF-223) on leave from the University of Texas Dental Branch, Houston, as research associate in anatomy, Harvard School of Dental Medicine (1958–59).

8 August 1959

Application of the Network Model to Gas Diffusion in Moist Porous Media

Abstract. Millington's description of pore structure in porous media is compared with conclusions based on the network theory. Experimental gas-diffusion data for moist sand indicate that this porous material has a network structure in which each pore is connected to about 15 other pores.

Millington (*1*) has recently presented a theory from which he derives a relation between gas diffusion through moist porous media and the moisture content of the material. His theory is based on a consideration of the planar distribution of spherical pores and the interconnection of pores in two adjacent planes. Millington uses Taylor's experimental data (*2*) to establish the validity of his theory.

The purpose of this report is to point out that Taylor's experimental data can be used to support a different theoretical treatment of pore structure in porous media. This treatment, based on the network model of a porous material (*3*), gives more detailed information on pore structure than does Millington's theory.

Although Millington limits himself to a discussion of diffusion through the gas space in dry and moist porous media, the same theory and equations apply to electrical conduction through electrolyte-containing porous media (*4,5*). The following equivalences can be shown to exist because of the equivalence of Ohm's law and Fick's first law of diffusion. (i) Steady-state diffusion of gas through a dry porous medium is governed by the same type of equation as is electrical conduction through a porous medium saturated with electrolyte. (ii) Steady-state diffusion of gas through a moist porous medium is governed by the same type of equation as is electrical conduction through a porous medium which contains a nonconducting fluid (oil) as the wetting phase and an electrolyte as the nonwetting phase. A brief, but perhaps oversimplified, definition of wetting phase is that it is the fluid phase which is spread on the internal surface of the porous material; conversely, the nonwetting phase is the fluid phase which occupies only the central portion of each pore space. In moist sand or soil the nonwetting phase is air and the wetting phase is water. If the porous material is exposed to the vapors of an organosilane, its surface will become hydrophobic. Water, or an electrolyte, will then be the nonwetting phase, while gas or oil is the wetting phase.

I have previously shown (*3*) that by treating a porous medium as a network of interconnected tubes, a relation can be obtained between electrical conductance and fraction of pore space occupied by a nonwetting electrolyte. This relation was shown to be dependent on the extent of interconnection of the tubes (pores) in the network, but independent of the pore size distribution.

To facilitate comparison of Millington's theory, the network theory, and Taylor's experimental data, it was desirable to state the diffusion coefficient and the moisture content relative to the dry porous material. In Fig. 1, D_M/D_d is the effective diffusion coefficient for gas in moist porous sand divided by the effective diffusion coefficient in the same sand when dry. The air-filled-pore volume is given as a fraction of the total pore volume.

Figure 1 shows a comparison of Millington's theoretical results, Taylor's experimental data, and the results from network models in which there are ten, seven, and four pores, respectively, connected to each pore. It is apparent from Fig. 1 that the network model predicts a relation between effective diffusion coefficient and moisture content that is slightly better than the one obtained by Millington. The network model in which each pore is connected to ten others gives results that are in fair agreement with Taylor's experimental data. From the trend of the network-model results, it seems reasonable to expect that the relationship of the effective diffusion coefficient versus the moisture content from a network in which each pore is connected to about 15 other pores will be in almost perfect agreement with the experimental data.

This observation gives support to the conclusion I had reached previously (*3*) by comparing data on experimental wetting-phase electrical conductivity with predictions from the network model. From my earlier work I concluded that the characteristic shape of a plot of experimental electrical conductivity in the wetting phase versus moisture content was a result of the network structure of porous media. Furthermore, the numerical value of these experimental data, when compared to predictions from the network model, suggested that in materials such as sand there are seven to 25 pores connected to each pore. Both Taylor's

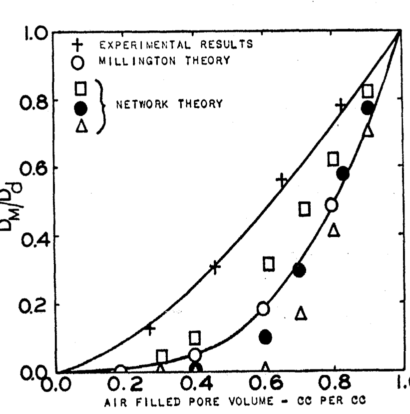

Fig. 1 Gas diffusion in a porous solid-liquid-gas system—a comparison of Taylor's experimental results (*2*), Millington's theory (*1*), and network theory (*3*). Number of pores connected to each pore in the network are: squares, 10; solid circles, 7; and triangles, 4.